Near-infrared electro-optic modulator based on silicon-graphene hybrid structure

Ciyuan Qiu, Ting Pan, and Yikai Su

State Key Lab of Advanced Optical Communication Systems and Networks, Department of Electronic Engineering,
Shanghai Jiao Tong University, Shanghai 200240, China
Author e-mail address: qiuciyuan@sjtu.edu.cn;yikaisu@sjtu.edu.cn

Abstract: Graphene has strong electro-optic effect which can be used to enhance the modulation efficiency of nanoscale photonic circuit. This paper describes recent developments for near-infrared electro-optic modulator based on silicon-graphene hybrid structure.
OCIS codes: (070.6120) Spatial light modulators; (070.5753) Resonators; (350.4238) Nanophotonics and photonic crystals

1. Introduction

Electro-optic modulator with high efficiency, operation speed and capability of large scale integration is a key technology required for future optical communications and computing. However, in nanoscale photonic circuit, it is challenging to achieve high modulation efficiency due to the inherently short light-matter interaction length. Therefore, researchers take great efforts in finding new materials with ultra-strong electro-optic effects or novel schemes to effectively enhance light intensity within a small volume [1].

Graphene, a sheet of carbon atoms in a hexagonal lattice, has attracted great interest recently. It has photon-like massless and gapless electrons which can strongly couple with light and exhibits wavelength-independent interband absorption (~2.3% per layer) in the visible range [2]. In the communication band, this universal absorption can be changed by tuning the Fermi level (E_f) of graphene through electric gating [3-5]. For instance, if light has a wavelength of 1.55 μm, i.e. photon energy $E_p = \hbar\omega$ is of 0.86 eV, the interband absorption can be blocked if $2E_f > E_p$. Such ultra-wide band tunability as well as ultra-high electron mobility make graphene a promising material to build active optoelectronic devices for high-speed communications. Recently, some near-infrared electro-optic modulators have been demonstrated based on silicon-graphene hybrid structure, including a silicon waveguide structure [3], a photonic crystal cavity [1] and a micro-ring resonator [5].

In this paper, we propose a spatial light modulator (SLM) and a nanobeam modulator based on silicon-graphene hybrid structures. Both of these two devices have modulation depths larger than 10 dB by FDTD simulations, while the modulation speeds are expected to be higher than 80 GHz. The high-speed silicon graphene hybrid spatial light modulator could be useful in 3D optical computing, imaging, display, holography, and so on [6]. Furthermore, the high-speed silicon-graphene hybrid nanobeam modulator is useful in dense wavelength division multiplexed (WDM) systems since it only has one resonance wavelength in the communication band, thus allowing other optical carriers in WDM systems to pass through the device without being affected.

2. Spatial light modulator

The SLM is constructed by a one-dimensional (1D) photonic crystal (PhC) cavity as shown in Fig. 1a. The 1D PhC is formed by periodic silicon ribs on a thin silicon slab, designed for the TE mode. The height of the silicon slab is 50 nm; the height of the silicon ribs is 220 nm, and its length is 4 μm (z direction shown as the yellow dashed line). The graphene is then transferred to this structure after depositing 10 nm Al_2O_3 by chemical vapor deposition (CVD).
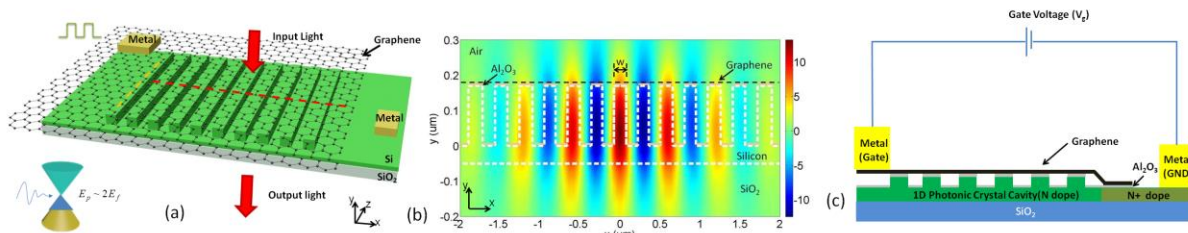

Fig. 1. a) Diagram of the SLM design where the graphene is located on top of silicon 1D photonic crystal cavity. Lattice constant of the PhC changes from 340 nm outside of the cavity to 290 nm at the center in 7 periods. b) E_z distribution corresponding to the red dashed line in (a). Here white dash line marks profile of silicon rib and slab region. Z direction is parallel to the length of the silicon ribs. c) Cross-sectional diagram of the modulator corresponding to the red dashed line in (a). The Fermi level of the graphene can be tuned by applying gate voltage between the graphene and the N+ doping regions.

The high Q cavity mode is achieved by adjusting the lattice constant and thus the bandgap of the PhC [6]. Fig. 1b shows E_z distribution of the cavity mode at cross section corresponding to the red dashed line in Fig. 1a. One can find that E_z has opposite signs in the neighboring ribs. To couple normal incident light into the cavity, one can introduce perturbation by increasing the width of the silicon ribs (represented as w in Fig. 1b) by Δw (in the x direction) where $E_z>0$, and decreasing the width of the silicon ribs by Δw where $E_z<0$. Note that the width perturbation of Δw is only applied in the cavity area where the lattice constant of the PhC is reduced. Then perturbation polarization $\Delta \vec{P} = \Delta w \cdot \vec{E}$ always points to the same direction and causes strong vertical radiation. Given the reciprocity in optics, the reverse process couples a normal incident optical beam into the resonator [6].

The resonant wavelength and the quality factor of cavity mode can be changed by tuning the Fermi level of the graphene through electric gating shown as in Fig. 1c. Here we begin with the gate-dependent permittivity of graphene to illustrate the principle. By using random phase approximation and Kramers-Kronig relation [7], gate-dependent permittivity of graphene has been extensively studied. The imaginary part, ε''_g , is characterized by interband and intraband absorptions while the real part, ε'_g , can be obtained by using Kramers-Kronig relation. The permittivity of the graphene can be expressed in following form:

$$\varepsilon_g{}'(E_p) = 1 + \frac{e^2}{8\pi E_p \varepsilon_0 d} \ln \frac{(E_p + 2|E_f|)^2 + \Gamma^2}{(E_p - 2|E_f|)^2 + \Gamma^2} - \frac{e^2}{\pi \varepsilon_0 d} \frac{|E_f|}{E_p^2 + (1/\tau)^2} \; , \tag{1}$$

$$\varepsilon_g{}''(E_p) = \frac{e^2}{4 E_p \varepsilon_0 d}[1 + \frac{1}{\pi}(\tan^{-1}\frac{E_p - 2|E_f|}{\Gamma} - \tan^{-1}\frac{E_p + 2|E_f|}{\Gamma})] + \frac{e^2}{\pi \tau E_p \varepsilon_0 d}\frac{|E_f|}{E_p^2 + (1/\tau)^2} \; , \tag{2}$$

where d is the thickness of graphene (0.5 nm), Γ is the interband linewidth broadening set to 160 meV. Since free carrier scattering rate $1/\tau$ is much smaller than the incident photon frequency ω, $1/\tau$ can thus be neglected. Fig. 2a shows the variation for the real part and imaginary part of the permittivity if the Fermi level is tuned. One can find the real part peak at $E_f = 0.4$ eV. If E_f is larger than 0.47 eV, the sign of the real part of permittivity becomes negative and the graphene shows its metallic properties. If the Fermi level increases, the imaginary part decreases, indicating the suppression of the interband absorption.
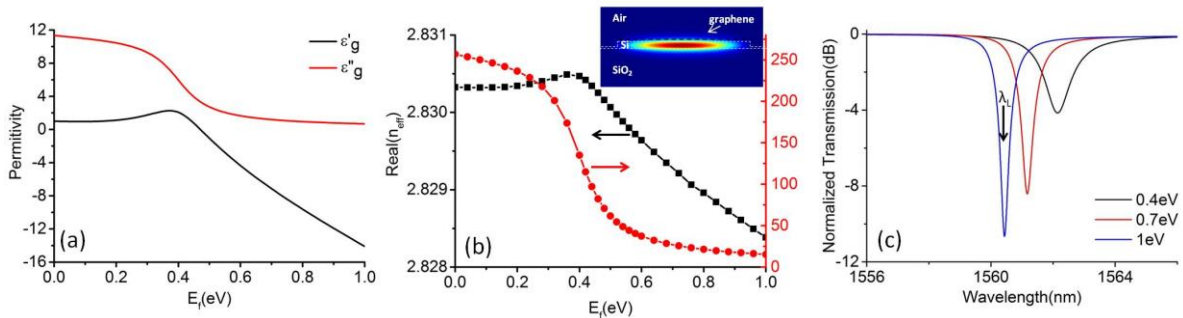

Fig. 2. a) Permittivity for the graphene under different Fermi level b) Real part of the effective index and loss for the silicon-graphene hybrid waveguide. Inset figure shows electrical field distribution for the silicon-graphene hybrid waveguide. The width of the silicon core is 4 μm while the height is 220 nm. The thickness of slab is 50 nm. c) Transmission spectra under different Fermi levels.

The inset of Fig. 2b shows electrical field distribution at the cross section of the silicon-graphene hybrid rib corresponding to the yellow dashed line in Fig. 1a. There is about 0.07% power located in the graphene layer. As light in the silicon core is evanescently coupled to the graphene layer, the permittivity of the graphene has large influence on the effective index of the hybrid waveguide (n_{eff}). The variation of n_{eff} is calculated from the Eigen-mode solver of the commercial software COMSOL. As shown in Fig. 2b, the real part of n_{eff} peaks at $E_f = 0.4$ eV, which matches the variation trend for the permittivity of graphene. To get better understanding of the imaginary part, we convert the imaginary part of n_{eff} to the loss of waveguide by wave propagation equation as Loss(dB/cm) = 4.3 × $2\pi / \lambda \times \mathrm{imag}(n_{eff}) / 100$. As shown in Fig. 2b, the loss of the waveguide decreases from about 250 dB/cm to 15 dB/cm if E_f increases from 0.4 eV to 1 eV. Since the real part of n_{eff} determines the resonant wavelength while the loss determines the quality factor of the cavity mode, we can thus change both the resonant wavelength and the quality factor of the cavity mode by tuning the Fermi level. The transmission spectra of the cavity mode under different Fermi levels are shown in Fig. 2c. The resonant wavelength is blue shifted by about 1.71 nm if the Fermi level increases from 0.4 eV to 1 eV. Both the quality factor and the extinction ratio increase due to the suppression of the interband absorption. If the operation wavelength λ_L is set to 1560.45 nm, the modulation depth is expected to

be larger than 10 dB. The capacitance from the graphene layer can be calculated to be ~ 0.1 pF. Thus the speed calculated as $1/2\pi RC$ can be as high as ~ 80 GHz by assuming R of 20 Ω [5].

3. Nanobeam modulator

The schematic of the nanobeam modulator is shown in Fig. 3a. Here the height of the silicon rib is 220 nm and the width of the nanobeam is 500 nm. Travelling light in the input waveguide can evanescently couple to the nanobeam resonator. The nanobeam resonator contains two reflector regions in the two sides and one taper region in the middle as shown in Fig. 3a [8]. The reflectors guarantee that light be highly reflected within the wavelength range of interest. The taper section is designed to smoothen the reflected optical response. The gap between the nanobeam resonator and the input waveguide is set to 167 nm to achieve the critical coupling condition if E_f = 1 eV. The gate voltage can be applied between the bottom n+ doped silicon slab and the graphene layer to tune the Fermi level of the graphene as shown in Fig. 3b. The modulator footprint mostly comes from the electrical contacts and the overall footprint can be down to ~20 μm^2.
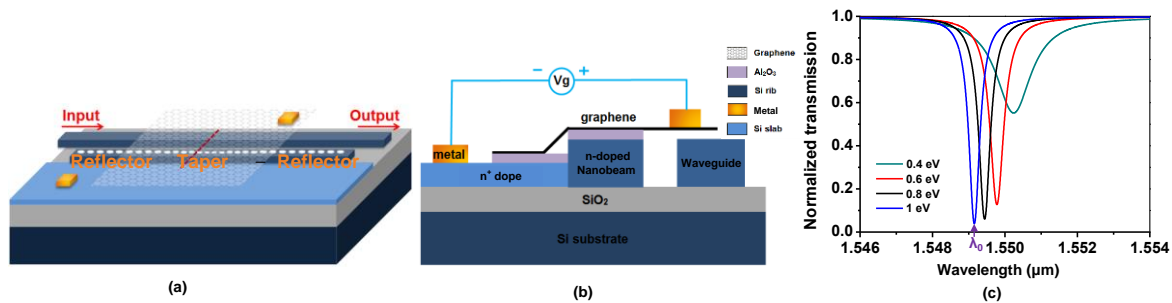

Fig. 3. a) Schematic perspective view of the proposed nanobeam modulator. b) The cross section corresponding to the red dashed line in (a). The thickness of Al_2O_3 is 7nm. c) Transmission spectra under different Fermi levels

Fig. 3c shows transmission spectra of the proposed device under different Fermi levels. Similar to the results discussed in section 2, both the real part and the imaginary part of the effective index for the silicon-graphene hybrid waveguide can be changed. If the Fermi level increases from 0.4eV to 1eV, transmission spectrum blue-shifts by about 1.09 nm, while the quality factor and extinction ratio increase due to the suppression of the interband absorption. Strong amplitude modulation depth as high as ~13.5 dB at λ_0 = 1549.2 nm is achieved. In our device, the graphene resistance is around 20 Ω and the capacitance is 60 fF, leading to a modulation speed of ~133 GHz.

4. Conclusion

We proposed an SLM and a nanobeam modulator using silicon-graphene hybrid structures. Based on FDTD simulations and theoretical calculations, the two devices are expected to operate at speeds higher than 80 GHz, with modulation depths larger than 10 dB. They may show applications in optical communication, optical computing, and so forth.

5. Acknowledgements

6. References

[1] A. Majumdar, J. Kim, J. Vuckovic, and F. Wang, "Electrical Control of Silicon Photonic Crystal Cavity by Graphene," Nano Letters,**13**, 515-518 (2013).
[2] R. R. Nair, P. Blake, A. N. Grigorenko, K. S. Novoselov, T. J. Booth, T. Stauber, N. M. R. Peres, and A. K. Geim, "Fine structure constant defines visual transparency of graphene," Science,**320**, 1308-1308 (2008).
[3] M. Liu, X. B. Yin, E. Ulin-Avila, B. S. Geng, T. Zentgraf, L. Ju, F. Wang, and X. Zhang, "A graphene-based broadband optical modulator," Nature,**474**, 64-67 (2011).
[4] F. Wang, Y. B. Zhang, C. S. Tian, C. Girit, A. Zettl, M. Crommie, and Y. R. Shen, "Gate-variable optical transitions in graphene," Science,**320**, 206-209 (2008).
[5] C. Y. Qiu, W. L. Gao, R. Vajtai, P. M. Ajayan, J. Kono, and Q. F. Xu, "Efficient Modulation of 1.55 mu m Radiation with Gated Graphene on a Silicon Microring Resonator," Nano Letters,**14**, 6811-6815 (2014).
[6] C. Y. Qiu, J. B. Chen, Y. Xia, and Q. F. Xu, "Active dielectric antenna on chip for spatial light modulation," Scientific Reports,**2**, (2012).
[7] J. Kim, H. Son, D. J. Cho, B. S. Geng, W. Regan, S. F. Shi, K. Kim, A. Zettl, Y. R. Shen, and F. Wang, "Electrical Control of Optical Plasmon Resonance with Graphene," Nano Letters,**12**, 5598-5602 (2012).
[8] W. S. Fegadolli, J. E. B. Oliveira, V. R. Almeida, and A. Scherer, "Compact and low power consumption tunable photonic crystal nanobeam cavity," Optics Express,**21**, 3861-3871 (2013).